Mechanism and kinetics of protein transport in chromatographic media studied by confocal laser scanning microscopy
Part II. Impact on chromatographic separations

Jürgen Hubbuch [a,*], Thomas Linden [b], Esther Knieps [a],
Jörg Thömmes [c], Maria-Regina Kula [a]

[a] *Institut für Enzymtechnologie, Heinrich-Heine Universität Düsseldorf, 52426 Julich, Germany*
[b] *Vaccine Bioprocess R&D, Merck & Co. Inc., Sumneytown Pike, West Point, PA 19486-0004, USA*
[c] *IDEC Pharmaceuticals Corp., 11011 Torreyana Road, San Diego, CA 92121, USA*

Abstract

The impact of different transport mechanism on chromatographic performance was studied by confocal laser scanning microscopy (CLSM) for solutions containing bovine serum albumin (BSA) and monoclonal IgG 2a under different solid- and fluid-phase conditions. During this investigation, a clear influence of the uptake mechanism on the affinity of the respective proteins for the different adsorbents and thus separation performance of the chromatographic process could be observed. For the system SP Sepharose[TM] Fast Flow at pH 4.5 pore diffusion could be ascribed to be the dominant transport mechanism for both proteins and the adsorption profiles resembled a pattern similar to that described by the 'shrinking core' model. Under these conditions a significantly higher affinity towards the adsorbent was found for BSA when compared to IgG 2a. With changing fluid- and solid-phase conditions, however, a change of the transport mode for IgG 2a could be detected. While the exact mechanism is still unresolved it could be concluded that both occurrence and magnitude of the now governing transport mechanism depended on protein properties and interaction with the adsorbent surface. For the system SP Sepharose[TM] XL at pH 5.0 both parameters leading to the change in IgG 2a uptake were combined resulting in a clear change of the system affinity towards the IgG 2a molecule, while BSA adsorption was restricted to the most outer shell of the sorbent.
© 2003 Elsevier B.V. All rights reserved.

Keywords: Confocal laser scanning microscopy; Composite media; Ion exchange; Protein transport; Proteins

1. Introduction

Productivity of preparative chromatographic processes is directly related to adsorption equilibrium and kinetics of the respective target proteins. Additionally, short processing times might diminish possible degradation of the product. There is, however, an inverse relationship between throughput and achievable capacities due to restrictions arising from intra-particle transport. Recent developments in the design of adsorbent structures aim therefore predominantly at an enhancement of intra-particle transport and/or protein capacities [1,2]. The employed resins are characterised by a combination of macro pores allowing convective fluid transport through the adsorbent and a network of micro pores of high surface area where diffusional transport is dominating [3,4]. A different approach was followed during the development of so called composite media [1]. These media consist of a rigid base matrix providing the stability necessary during column chromatography, while the pores are filled with a ligand carrying polymeric structure in order to enhance accessibility of binding sites and thus capacity. According to the loss of available pore space the latter would be expected to generate a greater pore transport resistance and therefore lower uptake rates. Studies evaluating adsorption behaviour and uptake kinetics, however, revealed that under certain conditions higher product capacities could be combined with a significantly enhanced uptake rate [2,6,7].

This behaviour was initially attributed to a change in the governing transport mechanism for which parameters such

* Corresponding author. Tel.: +49-2461-614173;
fax: +49-2461-612490.
E-mail address: j.hubbuch@fz-juelich.de (J. Hubbuch).

as the characteristic charge of the protein, the ability for multiple site interaction with the matrix or the bound protein concentration are discussed [5,8]. The true functionality and mechanism of this protein uptake pattern, however, is still unresolved. This lack of information is directly related to the fact, that traditional adsorption studies are based on the analysis of the protein concentration in the fluid phase in order to describe adsorption of protein to the stationary phase. This indirect analytical method for the evaluation of protein adsorption in porous adsorbents, however, results in data describing only the net result of a multiplicity of processes occurring within the adsorbent. In order to resolve these processes a variety of different mathematical models have been developed assuming different modes of transport or driving forces [9–11]. These models are mostly based on theoretical considerations supplemented by findings from related fields of research such as for example gas adsorption [12]. The applicability of these models, however, could not be verified by experimental data due to a lack of appropriate analytical methods.

A method to resolve single processes within the adsorbent by direct and quantitative analysis of intra-particle adsorption profiles has recently been developed and promises a new level of understanding of chromatographic processes. The method is based on the detection of fluorescently labelled protein molecules bound within adsorbent particles by confocal laser scanning microscopy (CLSM) [13–17]. With this method it is not only possible to detect the net adsorption profiles but also to analyse further transport of initially adsorbed protein molecules [6,17]. For the first time it was possible to directly evaluate the influence of pH and ionic strength on the transport and adsorption behaviour of BSA on a cation exchanger [17] and to show that under certain conditions BSA adsorption could be adequately described by the shrinking core model. This model has been developed to describe the adsorption of gas on solid surfaces and is based on pore diffusion as the governing transport mechanism [12,18]. When investigating the adsorption of IgG 2a to the cation exchangers SP Sepharose^{TM} Fast Flow and SP Sepharose^{TM} XL, it was found that the transport of a protein molecule might be governed by different transport mechanisms depending on adsorption conditions [6,17]. While the adsorption of IgG 2a on SP Sepharose^{TM} Fast Flow at pH 4.5 showed a behaviour similar to that described by the shrinking core model, a significantly different transport and adsorption behaviour has been found for SP Sepharose^{TM} Fast Flow at pH 5.0 and SP Sepharose^{TM} XL at pH 4.5 and 5.0 [6]. The latter being in accordance with reports on a variety of other proteins and solid phases [19,20]. The mechanism, on which this transport is based, led to a much faster saturation of the adsorbent than what could be predicted by a transport mode solely based pore diffusion. In the most extreme case of the investigated conditions—SP Sepharose^{TM} XL at pH 5.0—it was found that IgG 2a ($\sim$148 kDa) was able to saturate the

adsorbent ($0.9Q_{max}$) more than 14 times faster than BSA ($\sim$68 kDa), while at the same time exhibiting an only 18% lower molar capacity than the more than two-fold smaller molecule [6]. A first theoretical evaluation of the processes behind this behaviour is given by several authors [21–24]. While the mathematical formulation of the responsible processes and the subsequent experimental verification is still under debate, the most likely explanation seems to be based on a combination of pore diffusion and a second mechanism with an putative electrokinetic origin.

The understanding of parameters leading to such a fast and molecular size independent transport mode could be of utmost importance for the development of chromatographic protein separations. In this paper we investigate the impact of the different transport mechanisms and protein–protein interactions on chromatographic process performance. The model adsorption system used in this study—a solution containing IgG 2a and BSA—more or less represents a typical situation found in the purification of monoclonal antibodies from mammalian cell culture, where BSA often is a major impurity, which is supplemented to the growth medium together with several growth factors. A newly designed micro-column is employed for online detection of the dynamic processes occurring inside the adsorbent during packed bed chromatography.

2. Materials and methods

2.1. Adsorbents, proteins and chemicals

Bovine serum albumin (BSA) with a purity of >98% was ordered from Sigma–Aldrich (Deisenhofen, Germany). The non-specified IgG 2a monoclonal antibody was a gift from Böhringer Ingelheim Pharma (Ingelheim, Germany). The fluorescent dyes monofunctional Cy5 and Alexa 488^{TM} were purchased from Amersham Biosciences (Uppsala, Sweden); and Molecular Probes (Leiden, The Netherlands), respectively. SP Sepharose^{TM} Fast Flow and SP Sepharose^{TM} XL were obtained from Amersham Biosciences. For all CLSM studies a size-fractionation of the chromatographic resins with a lower and upper limit of 80 and 100 μm was carried out. Other chemicals were obtained from commercial sources in pa—analytical quality.

2.2. Labelling and preparation of protein solutions

Protein/dye conjugates were prepared following protocols recommended by the manufacturers. The chosen protein/dye conjugates in this study were BSA-Alexa 488^{TM} and IgG 2a-Cy5. The degree of labelling (DOL) was determined to 0.6–0.8 and 0.4 for BSA and IgG 2a, respectively. The obtained protein solutions were further diluted by a factor 1:20
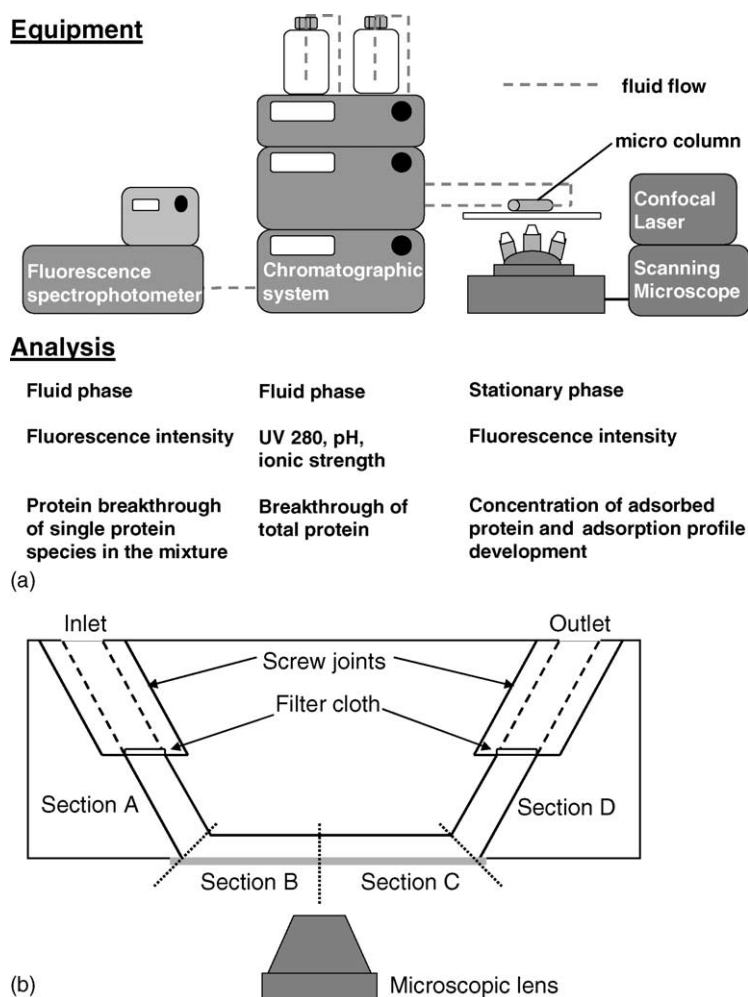
Equipment

Analysis

Fluid phase	Fluid phase	Stationary phase
Fluorescence intensity	UV 280, pH, ionic strength	Fluorescence intensity
Protein breakthrough of single protein species in the mixture	Breakthrough of total protein	Concentration of adsorbed protein and adsorption profile development

(a)

(b)

Fig. 1. (a) Experimental set-up during packed bed chromatography investigations. (b) Schematic drawing of the micro-column.

with unlabeled protein to adjust the fluorescent signal to a suitable level for the experimental conditions chosen [6].

2.3. Experimental set-up

A schematic drawing of the experimental set-up is given in Fig. 1a. The chromatographic process was controlled by an Äkta[TM] Basic 10 system (Amersham Biosciences). Microscopic analysis of the adsorption process within the chromatographic resin was carried out by a confocal laser scanning microscope (LSM 510, Zeiss, Göttingen, Germany). On-line analysis of the fluid composition leaving the micro-column was carried out by the Äkta[TM] system (UV 280) and a fluorescence spectrophotometer (Cary Eclipse, Varian, Victoria, Australia) equipped with an appropriate flow-cell cuvette (Type 176.753-QS, Helma, Mühlheim, Germany).

2.4. Micro-column design and handling

A schematic drawing of the employed micro-column is shown in Fig. 1b and a detailed description of the

micro-column design and its chromatographic performance can be found in Hubbuch et al. [25]. Briefly, the micro-column (inlet, window of observation, outlet) had a total length of 22 mm and a cross-sectional area of 3 mm^2 resulting in an effective column volume of 0.066 ml. The window of observation for the CLSM analysis was of approximately 8 mm in length and is situated in the middle of the column. For later analysis the column is divided in four different sections: the inlet (A), the front and end section of the window of operation (B) and (C), followed by the outlet (D). Prior to an experiment we equilibrated the packed bed in the column with 10-column volumes of the adsorption buffer used for the respective breakthrough analysis. A fluid velocity of 100 cm/h was used during equilibration and all subsequent experiments. All experiments were carried out using 50 mM acetate buffer at pH 4.5 and 5.0.

2.5. Fluid-phase analysis

The fluid leaving the micro-column was analysed both for total protein (UV 280) and for the content of the sin-

gle protein species present (fluorescence). In order to minimise bleed-through between detector channels and to avoid re-absorption of emitted light, the excitation and emission wavelength for the detection of Alexa 488[TM] (Ex.: 496 nm; Em.: 532 nm) and Cy5 (Ex.: 633 nm; Em.: 670 nm) were chosen according to the characteristics of the respective fluorophores. In order to ensure a linear relation between the concentration of labelled protein in solution and the fluorescence signal detected with the fluorescence spectrophotometer, a series of solutions with known concentrations was applied prior to an experimental run to define an appropriate detection range. During previous work no significant alterations in the adsorption behaviour between native and labelled molecules could be found for the systems employed in this study [17]. Additionally, a comparison between the breakthrough of total protein (UV 280) and the sum of the respective single component breakthroughs has been carried out. The extinction coefficients used for this evaluation were 0.671 and $1.351 \mathrm{g}^{-1} \mathrm{cm}^{-1}$ for BSA and mIgG 2a, respectively.

2.6. Detection of confocal images

Confocal images were detected employing a LSM510 Zeiss confocal laser scanning microscope. The microscope was equipped with separate pinholes for the investigated emission wavelengths and the two objective lenses Plan-Neofluar 40×/1.3 Oil and C-Apochromat 63×/1.2Wcorr were used. Multi-component scans were carried out in a sequential scan mode employing the following wavelength settings: Alexa 488[TM] (Ex.: 488 nm; Em.: 505–530 nm) and Cy5 (Ex.: 633 nm; Em.: 650 nm). Suitable laser intensity was chosen in order to provide a high signal-to-noise ratio and a loss of photo stability of less than 5% after 10 consecutive scans [25]. The scans over the cross-sectional area of the supports were carried out along the optical x–y-axes, i.e. horizontally. The appropriate z-value of the scanning coordinates was found by a simple experimental procedure prior to an experimental run [25].

2.7. Data evaluation

The information from the confocal images was extracted as published in detail earlier by calculating relative capacity values Q_{rel} from fluorescence intensity profiles generated over the scanned cross-sectional area of the adsorbent particle [25]. In brief, an average volumetric intensity of all pixels with a distance r_i to the center of the sorbent was determined and used to calculate the respective shell intensity. The sum over the various shell intensities divided by the support volume resulted in the relative capacity Q_{rel} of the examined adsorbent particle. The analysis of the CLSM pictures and following data treatment has been carried out by a custom-designed software package based on Visual Basic 6.0.

3. Results and discussion

3.1. Two-component adsorption

Fig. 2a–d shows the obtained breakthrough curves of total protein (UV 280) supplemented with the respective breakthrough curves of the two components BSA and IgG 2a measured off-line in the collected fractions by fluorescence spectrometry. The sum of the individual breakthrough curves corresponds well with the signal for total protein indicating that the adsorption behaviour of the labelled protein is analogous to that of the unlabeled protein fraction (see also Table 1). This is in accordance with previous studies [17].

3.2. Breakthrough behaviour

The 'affinity' of a protein for a chromatographic resin is to a large extent determined by the interaction strength between protein and the respective ligand as well as by the adsorbent structure. Breakthrough during frontal application, however, is a complex function of adsorption equilibrium and kinetics. In order to simplify such a complex analysis the breakthrough behaviour (of a 1:1 molar mixture of BSA and

Table 1
Dynamic breakthrough capacities of total protein and the individual proteins during chromatographic investigations

	SP Sepharose[TM] FF		SP Sepharose[TM] XL	
	pH 4.5	pH 5.0	pH 4.5	pH 5.0
$Q_{10\%, \mathrm{TP}}$ (mg/ml)[a]				
Total protein (UV 280)	30.61	58.3	51.8	29.3
Total protein (fluorescence)	28.8	53.77	63.9	28.2
BSA/IgG 2A	14.7/14.2	26.7/27.1	32.4/31.5	13.5/14.7
$Q_{10\%, \mathrm{Prot}}$ (mg/ml)[b]				
BSA	39.2	25.75	35.8	23.7
IgG 2A	13.9	29.5	31.5	52.5

All capacities were determined during breakthrough of a employing a 1:1 molar mixture of BSA and IgG 2a.
  [a] Capacities at 10% breakthrough of total protein.
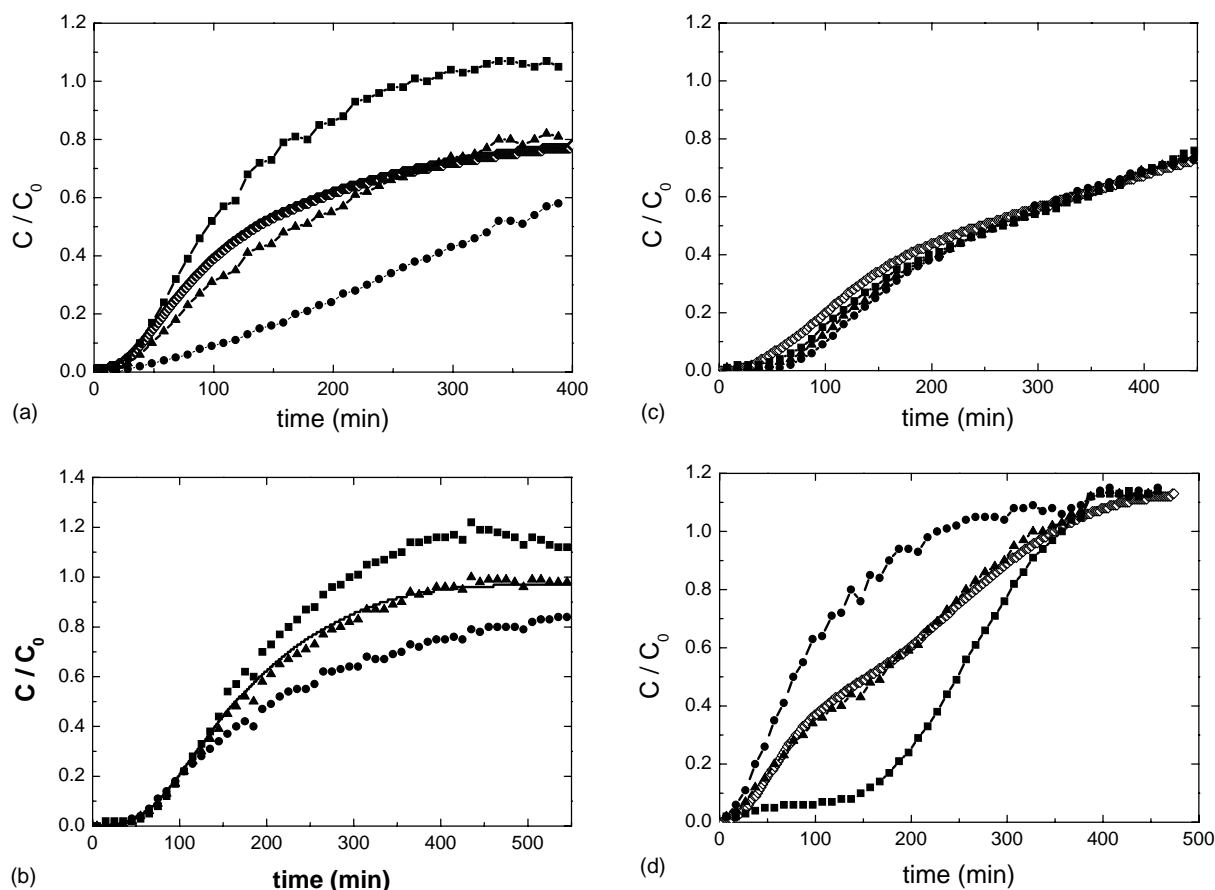 [b] Capacities for the single protein components at 10% breakthrough of the respective component.

Fig. 2. Breakthrough curves of an IgG/BSA solution (1:1, w/w). (a) SP Sepharose^{TM} FF at pH 4.5, (b) SP Sepharose^{TM} FF at pH 5.0 (taken from [25]), (c) SP Sepharose^{TM} XL at pH 4.5, (d) SP Sepharose^{TM} XL at pH 5.0. Key: (■) IgG, (●) BSA, (▲) IgG and BSA, (◇) total protein UV 280.

IgG 2a) shown in Fig. 2a–d is therefore initially described by the respective $Q_{10\%}$ values, representing the individual adsorbent capacity at 10% breakthrough. In the following we differentiate between sorbent capacity for the two components at 10% breakthrough of total protein $Q_{10\%, TP}$ and the adsorbent capacity for the individual component at 10% breakthrough of the respective component, $Q_{10\%, BSA}$ and $Q_{10\%, IgG 2a}$, within the two-component solution. All values are obtained during breakthrough studies employing a 1:1 molar mixture of BSA and IgG 2a. The values obtained under different conditions are shown in Table 1.

Comparing the breakthrough capacities for the single proteins—BSA and IgG 2a—at 10% breakthrough of total protein, $Q_{10\%, TP}$, similar capacities for BSA and IgG 2a were found within each system, which suggests at first glance that both species bind with approximately the same equilibrium and kinetics to the support. A clearer picture of the differences in affinity of the respective protein species towards the supports under different conditions and a possible link between the respective affinity and the $Q_{10\%, TP}$ value can be found when examining the binding capacity of the respective proteins not at 10% breakthrough of total protein but at 10% breakthrough of the single protein within the two-component solution.

The highest value for $Q_{10\%, BSA}$ of 39.2 mg/ml was obtained for SP Sepharose^{TM} Fast Flow at pH 4.5 combined with the lowest value for $Q_{10\%, IgG 2a}$ of 13.9 mg/ml. Under these conditions BSA binding is therefore clearly favoured. For SP Sepharose^{TM} XL at pH 5.0 this relationship is reversed leading to $Q_{10\%, Prot}$ values of ∼52.5 mg/ml for IgG 2a and ∼23.7 mg/ml for BSA indicating a higher affinity of the adsorbent for IgG 2a. The above conditions exhibiting a selectivity for one of the protein species are accompanied by a low dynamic capacity of total protein leading to a $Q_{10\%, TP}$ value of ∼30 mg/ml. For SP Sepharose^{TM} Fast Flow at pH 5.0 and SP Sepharose^{TM} XL at pH 4.5 a significantly higher dynamic capacity of total protein of 58.3 and 51.8 mg/ml was detected. This increase of dynamic capacity is, however, connected to a loss in 'affinity' for one of the protein species. For both conditions similar $Q_{10\%, Prot}$ values for BSA and IgG 2a were found.

Summarising the breakthrough behaviour shown in Fig. 2 and the respective 10% breakthrough capacities examined in this study, we obtain the following order of 'affinity' for BSA and IgG 2a:

$$\text{BSA}: \text{SP XL pH 5.0} \sim \text{SP FF pH 5.0}$$
$$< \text{SP XL pH 4.5} \sim \text{SP FF pH 4.5}$$

IgG 2a : SP FF pH 4.5 ≪ SP FF pH 5.0

   ∼ SP XL pH 4.5 ≪ SP XL pH 5.0

The order of 'affinity' found during the chromatographic separation of IgG 2a is in agreement with kinetic saturation data obtained during single component studies. Furthermore, the increase in affinity for the IgG 2a coincides with a change of the respective transport modes exhibited by the molecules for the various mobile and stationary-phase conditions [6].

3.3. Adsorption pattern

The close relationship between results obtained during single component studies and the chromatographic behaviour described above is consistent with the finding that the adsorption profile development detected during the two component study can simply be described as a combination of the profiles and thus transport mechanisms detected for the two components during single component studies under non-saturating conditions [6,17]. The respective adsorption profiles of BSA and IgG 2a are shown in Figs. 3–5. Superimposed to the respective adsorption and transport behaviour are interactions between the protein species such as displacement of one species by the other. This is demonstrated quantitatively in Fig. 6a–c where the fractional saturation of the single adsorbent particles is plotted as a function of time. Due to the dynamic nature of these adsorption studies we chose the maximal value Q_{max} of a protein species detected during the confocal investigation for normalizing the data. According to the results presented above and those found during single component studies [6,17,25] three distinct groups can be differentiated.

3.3.1. SP Sepharose^TM Fast Flow at pH 4.5

For adsorption on SP Sepharose^TM Fast Flow at pH 4.5, the dominating transport mode for both protein species—IgG 2a and BSA—can be attributed to pore diffusion and the obtained adsorption profiles resemble profiles similar to those described by the shrinking core model.

The confocal images reveal further that BSA adsorbs in a ring-wise fashion to the outer part of the adsorbent enclosing the earlier bound IgG 2a (see Fig. 3). After this ring of BSA reaches a certain thickness the amount of IgG 2a adsorbed in a single support seems to remain constant, i.e. no additional IgG 2a is bound to the adsorbent. Four confocal pictures were taken during the course of this experimental run indicating that the fractional saturations in sections B and C follow each other (see Fig. 6a). The capacity development of IgG 2a in section B seems to decrease after ∼150 min, i.e. IgG 2a is displaced by BSA. The true reason why no additional IgG 2a is adsorbed within the sorbent, however, is not yet clear. A restricted transport of IgG 2a due to pure sterical hindrance can be ruled out. From pore accessibility studies it became clear that the cross-sectional area of the pores even though reduced in size by the bound BSA should remain open enough to allow diffusion of molecules in the

size-range of the IgG 2a molecule [6]. It was furthermore shown during single component studies that under the investigated conditions newly arriving IgG 2a molecules are transported past the initially adsorbed layer of IgG 2a molecules. A more likely explanation of this effect might be related to the displacement of IgG 2a by BSA due to the higher affinity of BSA under these conditions combined with a higher diffusion constant for BSA. The diffusion constants for BSA and IgG in free solution were determined to 5.8×10^{-11} to 6.2×10^{-11} and 3.8×10^{-11} to 4.0×10^{-11} m^2/s, respectively [26].

3.3.2. SP Sepharose^TM Fast Flow at pH 5.0 and SP Sepharose^TM XL at pH 4.5

The transport and adsorption behaviour detected for SP Sepharose^TM Fast Flow at pH 5.0 [25] and SP Sepharose^TM XL at pH 4.5 is characterised by a combination of pore diffusional transport (BSA) and secondary transport (IgG 2a). The adsorption/transport of IgG 2a is characterised by both a higher capacity and faster transport when compared to Sepharose^TM Fast Flow at pH 4.5. In both cases the adsorption front detected for IgG 2a can be described by a positive concentration gradient of bound/accumulated molecules moving towards the center of the adsorbent followed by an 'overshoot' of bound/accumulated protein in the middle part of the support. The sharp leading edges of the protein front moving to the center of the particle might be explained by the spherical geometry of the adsorber. The latter providing less binding space as the proteins move towards the center leading to a concentration of the proteins which might accelerate the transport resulting in a self-sharpening effect. The decline of this overshoot is superimposed by a displacement of IgG 2a by BSA (see Fig. 6b and c). While the displacement of IgG 2a is near complete for SP Sepharose^TM Fast Flow at pH 5.0, we only detected a minor decrease in the fractional saturation for IgG 2a on SP Sepharose^TM XL at pH 4.5. This might be explained by a general higher 'affinity' of BSA towards the SP Sepharose^TM Fast Flow adsorbent combined with an increase of the affinity of IgG 2a for the XL adsorbent as compared to the Fast Flow adsorbent. This is consistent with data from single component studies [6] and is further underlined by the fact that BSA adsorption on SP Sepharose^TM XL at pH 4.5 is confined to the outer sections of the adsorber, while transport into the adsorber is restricted (see Fig. 4). The latter is regardless of the fact that BSA sorption should be favoured at pH 4.5 as we experience a shift of the net charge of BSA from positive to negative when going from pH 4.5 to 5.0. This shift in 'affinity' for different adsorbents might therefore only be attributed to the sorbent structure and the governing transport mechanism for the respective protein molecules.

Additionally, no clear restriction of the transport of IgG 2a into and within the adsorbent was detected, i.e. the transport of the IgG 2a molecule remains possible in the pore network after BSA adsorption. BSA is again adsorbing in a ring-wise fashion as described for SP Sepharose^TM Fast Flow at pH 4.5.
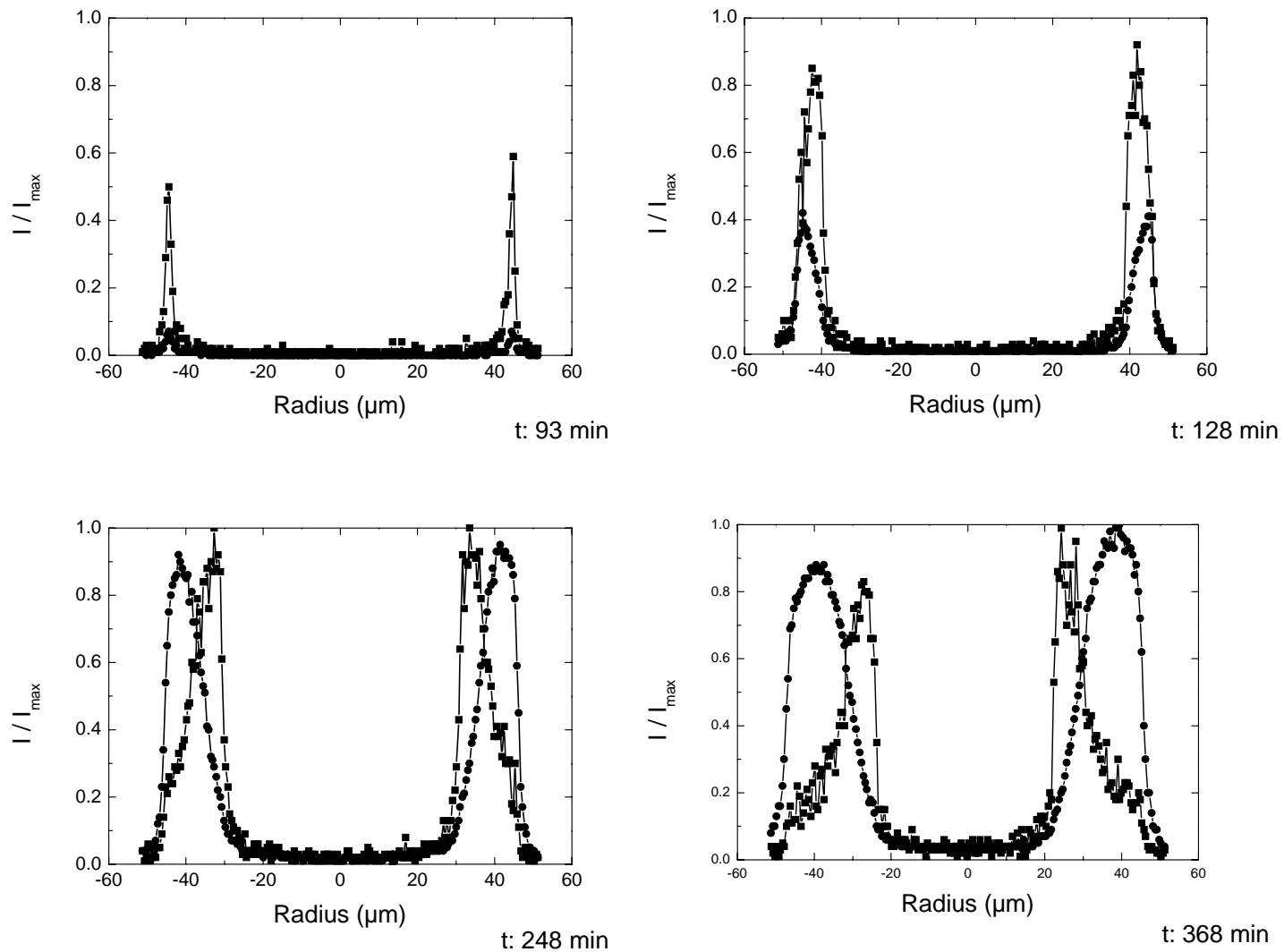
Fig. 3. Adsorption profiles of a 1:1 BSA (●) and IgG (■) mixture on SP Sepharose^TM FF at pH 4.5. The profiles were detected during breakthrough experiments (time scale added in the figure) using the micro-column.
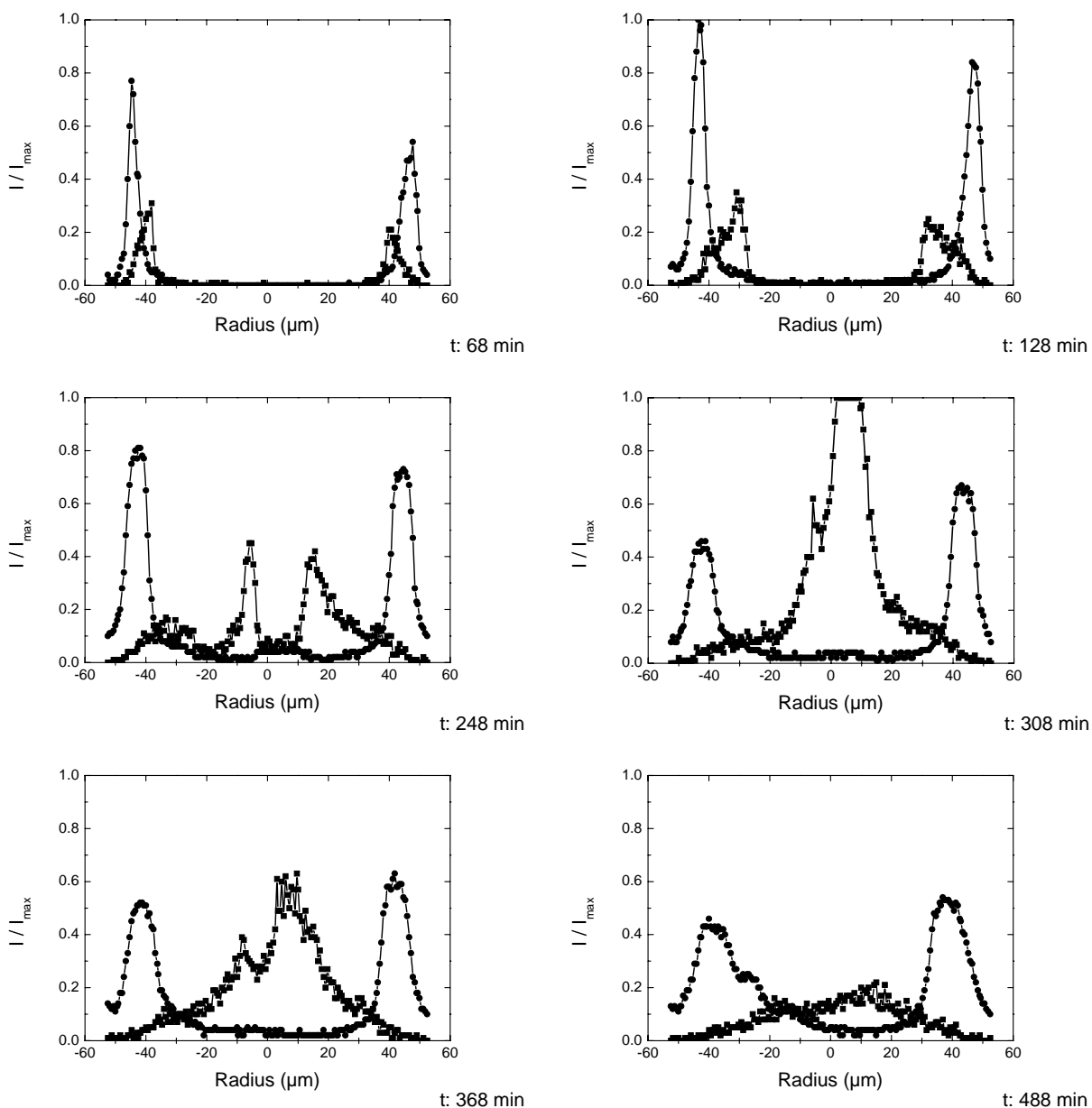
Fig. 4. Adsorption profiles of a BSA (●) and IgG (■) mixture on SP Sepharose[TM] XL at pH 4.5. The profiles were detected during breakthrough experiments (time scale added in the figure) using the micro-column.

Finally, it was found that the overshoot detected during IgG 2a adsorption is far stronger for the SP Sepharose[TM] XL adsorber than for SP Sepharose[TM] Fast Flow [25]. The results presented above indicate that the shift in the transport mechanism is influenced by both a change in the surface properties of IgG 2a by the increasing pH and a change of sorbent architecture, while the change of affinity from BSA to IgG 2a is closely connected to the sorbent architecture. A likely explanation might be related to the dextran network filling the pores, thus resulting in a distinct phase for IgG 2a adsorption and transport, which will be discussed below.

3.3.3. SP Sepharose[TM] XL at pH 5.0

For SP Sepharose[TM] XL at pH 5.0 we now combine the two enhancing effects for IgG 2a adsorption and transport detected during single component studies [6], namely a shift of protein surface properties and sorbent architecture. Accordingly we obtained the most significant separation of the two compounds over the length of the column (see Table 1). During the time span of 1 h we detected an increase of bound IgG 2a of approximately 64% distributed over the whole particle cross-section (see Figs. 5 and 6d). The high 'affinity' and fast intra-particle transport for IgG 2a is further underlined by the fact that for the first time we detected
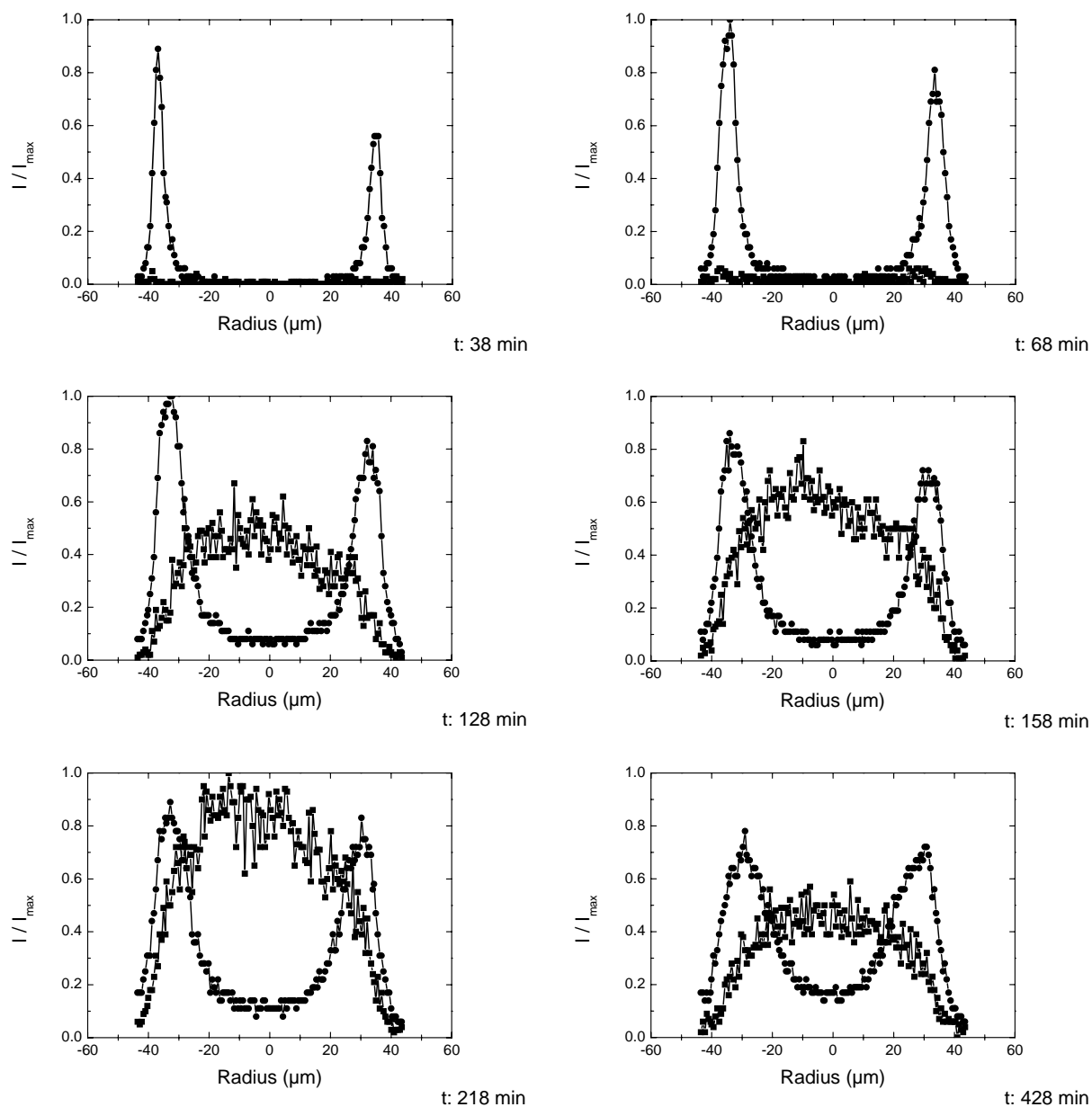
Fig. 5. Adsorption profiles of a BSA (●) and IgG (■) mixture on SP Sepharose[TM] XL at pH 5.0. The profiles were detected during breakthrough experiments (time scale added in the figure) using the micro-column.

BSA adsorption prior to IgG 2a adsorption (see Fig. 6d) indicating that the IgG 2a adsorption front within the bed is progressing slower than that of BSA. The initial adsorption of BSA followed by IgG 2a adsorption clearly demonstrates that IgG 2a transport was not restricted by already adsorbed BSA. Furthermore, the profile development detected for SP Sepharose[TM] Fast Flow at pH 5.0 and SP Sepharose[TM] XL at pH 4.5—an increase of the locally adsorbed IgG 2a towards the centre followed by an overshoot in the bound protein concentration in the middle of the support and a subsequent decline to an equilibrium value—could not be observed for SP Sepharose[TM] XL at pH 5.0. The adsorption profile could thus be rather described by a gradual increase

of adsorbed IgG 2a over the whole cross-sectional area, leading to a maximal capacity at ∼270 min followed by a slight decrease (see Fig. 5). This is consistent with findings during single component studies [6]. It is, however, not yet clear if the slight decrease in IgG 2a capacity towards the end of the breakthrough results from a displacement by BSA or the transport mechanism. The higher IgG 2a affinity for the Sepharose[TM] XL adsorbent structure and the additional restriction of BSA transport by the dextran network and adsorbed IgG 2a, however, strongly suggest the latter.

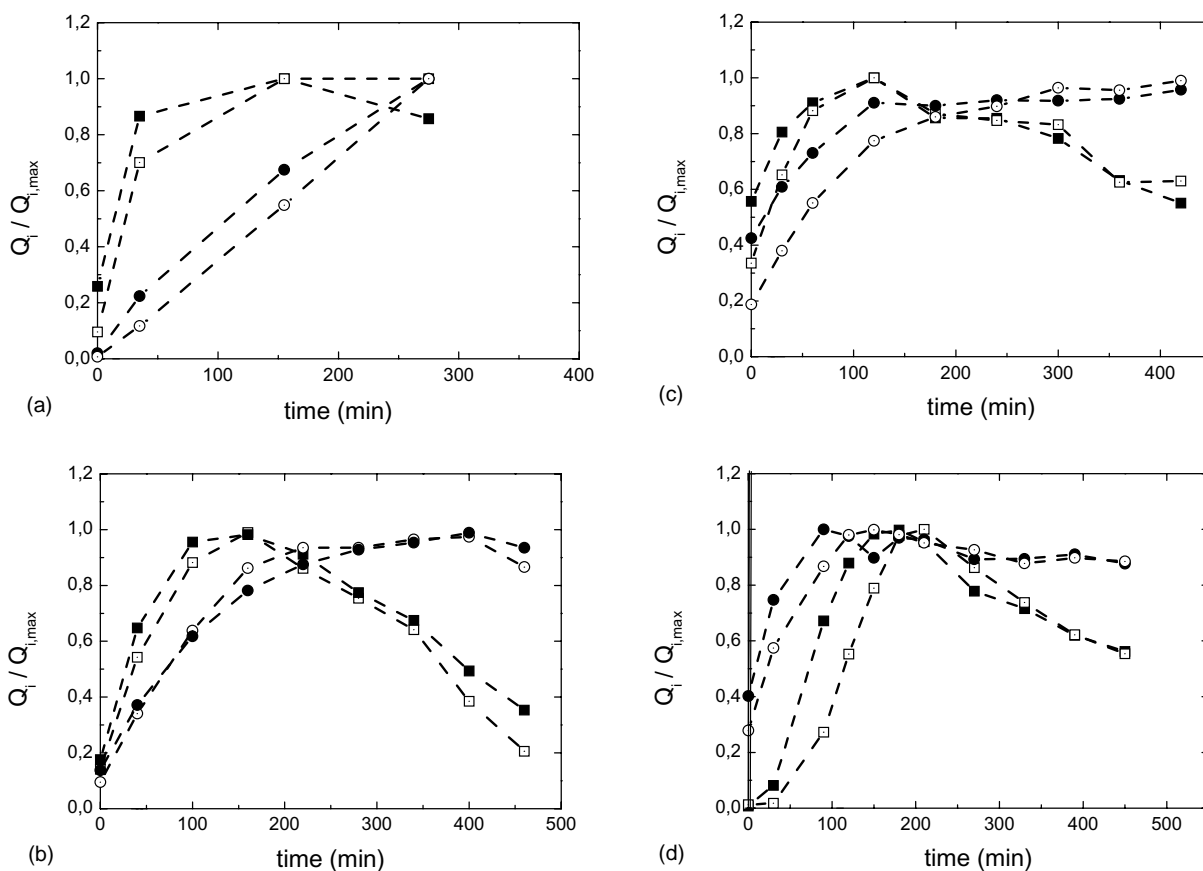A common theme of models aiming at the mechanistic description of the detected intra-particle profile propagation

Fig. 6. Relative amount of IgG (■, □) and BSA (●, ○) adsorbed in region B (closed symbols) and C (open symbols) of the column (see Fig. 1). The data points represent an average over four scanned positions. (a) SP Sepharose[TM] FF at pH 4.5, (b) SP Sepharose[TM] FF at pH 5.0, (c) SP Sepharose[TM] XL at pH 4.5, (d) SP Sepharose[TM] XL at pH 5.0.

is the combination of pore diffusion and a second mechanism with electrokinetic origin [19,20,22]. The extent of the latter responsible for the fast intra-particle transport described above. While the link between a change of surface properties and the susceptibility of a protein towards the non-diffusive transport mechanism is under debate, it became clear from the above results that the change in adsorbent structure and in the present case degree of available surface area had an effect on both the affinity for IgG 2a and the governing transport mechanism. The open pore structure and thus low degree of surface interactions for SP Sepharose[TM] Fast Flow seems to inhibit a switch to the non-diffusive transport mechanism while an increase of possible surface interactions—given by the SP Sepharose[TM] XL structure—let to a clear shift towards the putative electrokinetically based transport mechanism. As both adsorbents have an approximately similar ionic capacity and backbone structure it can be concluded that the better accessibility and distribution of the charges in the pore volume—given by the SP Sepharose[TM] XL structure—results in a more favourable situation for the electrokinetic based transport mechanism than the open pore structure but higher surface charge density given by SP Sepharose[TM] FF.

The necessary contribution of the SP Sepharose[TM] XL design at pH 4.5 could be related to some sort of multi-point attachment mechanism, which might act favourable for a switch to the non-diffusive transport mechanism of IgG 2a. It was furthermore shown that at pH 5.0 the time to reach 90% saturation for SP Sepharose[TM] XL was more than four times shorter than for SP Sepharose[TM] Fast Flow [6]. This is consistent with conclusions derived by Lewus and Carta [8] that the uptake behaviour is dependent on the protein surface properties as well as its ability to interact with multiple binding sites. When investigating another composite media, Weaver and Carta [2] argued further that the hydrogel used to fill the pore matrix could be treated as a form of matter intermediate between a solid and liquid [27] with the polymer chains being flexible and in constant thermal motion. Additionally, it was shown by Park et al. [28] that the hydrodynamic screening length in those adsorbers was too small to allow unhindered diffusion of proteins through a charged net of polymer chains and that the most likely occurrence would be a continuous interaction of the proteins with a multiplicity of functional groups. The active contribution of the flexible polymer chains in the pore phase might be further underlined by findings from Jeppensen et al. [29],

which indicate that ligand–receptor interactions of tethered systems cannot be solely based on the 'reach' of polymers in there equilibrium state but is more a function of dynamic fluctuations of the polymers where the stretching distance of these polymers turned out to be far longer than the average reach at equilibrium. The final answer to the contribution of the adsorbent architecture should, however, lie in the understanding of the change of driving forces within a composite media.

4. Summary and conclusions

A detailed study of the implications arising from variations in fluid- and solid-phase conditions on protein separation during chromatographic processes was carried out. The investigated system resembles a task normally faced when purifying monoclonal antibodies from cell culture supernatant. By carefully optimising mobile phase as well as stationary-phase conditions it was possible to clearly favour IgG 2a adsorption and transport, while the capacity for BSA—representing the contaminating fraction—could be significantly reduced.

Analysis based on confocal laser scanning microscopy revealed that the change of 'affinity' and sorption kinetics found for the investigated systems is closely related to the adsorbate structure and the susceptibility of the IgG 2a molecule towards a non-diffusive transport mechanism. This transport mechanism let to a faster intra-particle transport irrespective of the much higher molecular weight of the IgG 2a molecule when compared with BSA. From our studies it became clear that the shift of the governing transport mechanism from pore diffusions towards a putative electrokinetically based transport could be triggered by both, a change in mobile-phase conditions and thus properties of the protein molecule as well as stationary-phase conditions. While the exact mechanistic explanation of the observed intra-particle transport is under debate [21–24] it is clear that—in the light of the complexity of these systems, the number of involved parameters and the current density of experimental data—current models might point to the right direction and thus aid the design of experimental investigations but are far from a quantitative description of the observed phenomena.

An understanding of the physical parameters and the interplay between protein structure, mobile-phase parameters and stationary-phase architecture resulting in a change of the governing transport mechanism might, however, lead to new strategies for protein separation processes and custom-designed stationary phases.

References

[1] E. Boschetti, J. Chromatogr. A 658 (1994) 207.
[2] L.E. Weaver, G. Carta, Biotechnol. Progress 12 (1996) 342.
[3] N.B. Afeyan, N.F. Gordon, I. Mazsaroff, L. Varady, S.P. Fulton, J. Chromatogr. 519 (1990) 1.
[4] D. Whitney, M. McCoy, N. Gordon, N. Afeyan, J. Chromatogr. A 807 (1998) 165.
[5] R.K. Lewus, F.H. Altan, G. Carta, Ind. Eng. Chem. Res. 37 (1998) 1079.
[6] J. Hubbuch, T. Linden, E. Knieps, A. Ljunglöf, J. Thömmes, M.-R. Kula, J. Chromatogr. A 1021 (2003) 93–104.
[7] J. Thömmes, Biotechnol. Bioeng. 62 (3) (1999) 358.
[8] R.K. Lewus, G. Carta, AIChE J. 45 (3) (1999) 512.
[9] B.H. Arve, A.I. Liapis, AIChE J. 33 (1987) 179.
[10] A. Johnston, M.T.W. Hearn, J. Chromatogr. 557 (1991) 335.
[11] H. Yoshida, M. Yoshikava, T. Kataokal, AIChE J. 40 (1994) 2034.
[12] D.M. Ruthven, Principles of Adsorption and Adsorption Processes, Wiley, New York, 1984.
[13] A. Ljunglöf, R. Hjorth, J. Chromatogr. A 743 (1996) 75.
[14] A. Ljunglöf, J. Thömmes, J. Chromatogr. A 813 (1998) 387.
[15] T. Linden, A. Ljunglöf, M.R. Kula, J. Thömmes, Biotechnol. Bioeng. 65 (6) (1999) 622.
[16] T. Linden, K. Lacki, A. Ljunglöf, J. Thömmes, AIChE J. (2003) in press.
[17] T. Linden, A. Ljunglöf, L. Hagel, M.R. Kula, J. Thömmes, Sep. Sci. Technol. 37 (1) (2002) 1.
[18] S. Yagi, D. Kunii, in: Proceedings of the Fifth Symposium on Combustion, Nostrand Reinhold, New York, 1955.
[19] T. Linden, Untersuchungen zum inneren Transport bei der Proteinadsorption an poröse Medien mittels konfokaler Laser-Raster-Mikroskopie, Doctoral Thesis, Heinrich-Heine-Universität Düsseldorf, 2001.
[20] A. Ljunglöf, Direct Observation of Biomolecule Adsorption and Spatial Distribution of Functional Groups in Chromatographic Adsorbent Particles, Doctoral Thesis, Uppsala University, http://www.uu.se/avhandlingar, 2002.
[21] A.I. Liapis, B.A. Grimes, K. Lacki, I. Neretnieks, J. Chromatogr. A 921 (2) (2001) 135.
[22] B.A. Grimes, A.I. Liapis, J. Colloid Intref. Sci. 248 (2002) 504.
[23] C. Martin, G. Iberer, A. Ubiera, G. Carta, ISPPP 2002, Heidelberg, 10–13 November 2002.
[24] S.R. Dziennik, E.B. Belcher, G.A. Barker, M.J. DeBergalis, S.E. Fernandez, A.M. Lenhoff, PNAS 100 (2) (2003) 421.
[25] J. Hubbuch, T. Linden, E. Knieps, J. Thömmes, M.R. Kula, Biotechnol. Bioeng. 80 (4) (2002) 359.
[26] M.T. Tyn, T.W. Gusek, Biotechnol. Bioeng. 35 (1990) 327.
[27] T. Tanaka, Sci. Am. 224 (1981) 124.
[28] H.H. Park, C.S. Johnnson, D.A. Gabriel, Macromolecules 23 (1990) 1548.
[29] C. Jeppesen, J.Y. Wong, T.L. Kuhl, J.N. Israelachvili, N. Mullah, S. Zalipsky, C.M. Maerques, Science 293 (1991) 465.